



Universiteit
Leiden
The Netherlands

Search for cosmic neutrinos with ANTARES

Bogazzi, C.

Citation

Bogazzi, C. (2014, May 15). *Search for cosmic neutrinos with ANTARES. Casimir PhD Series*. Retrieved from <https://hdl.handle.net/1887/25771>

Version: Corrected Publisher's Version

License: [Licence agreement concerning inclusion of doctoral thesis in the Institutional Repository of the University of Leiden](#)

Downloaded from: <https://hdl.handle.net/1887/25771>

Note: To cite this publication please use the final published version (if applicable).

Cover Page



Universiteit Leiden



The handle <http://hdl.handle.net/1887/25771> holds various files of this Leiden University dissertation.

Author: Bogazzi, Claudio

Title: Search for cosmic neutrinos with ANTARES

Issue Date: 2014-05-15

4. Simulation and reconstruction

We can only see a short distance ahead, but we can see plenty there that needs to be done.

Alan Turing

In this chapter, the simulation of the signal and the background is described and the track reconstruction algorithm used in the analysis is presented. First, the trigger algorithms responsible for data filtering are introduced in Section 4.1. Section 4.2 presents the Monte Carlo tools: event generation and detector response. Finally, Section 4.3 focuses on the muon track reconstruction.

4.1. Triggers

All the hits exceeding a pre-defined threshold, typically the equivalent of 0.3 single photo-electrons (L0 hits) are sent to shore where they are filtered by a farm of PCs. This results in a transfer of several Gb/s to shore. Most of the hits are due to optical background from ^{40}K decays or bioluminescence. Optical background hits are uncorrelated and induce primarily single photo-electrons hits. Hence, a first filtering is done by requiring hits with a high charge (usually > 3 photo-electrons) or coincident hits within a time window of 20 ns on separate PMTs of the same storey. Hits satisfying these criteria are called "L1 hits". With this first selection, the amount of data is reduced by a factor of 10^2 [132].

Hits originating from the same muon normally fulfill the "causality" criterion:

$$|\Delta t| \leq \frac{c}{n_g} \cdot d + 20 \text{ ns} \quad (4.1)$$

where Δt is the time difference between two hits, d is the distance between the two PMTs which have recorded the two hits and c/n_g is the group velocity of light in sea water. An additional ± 20 ns is added to this time window to account for possible time calibration uncertainties and light scattering. A set of L1 hits which satisfies Equation 4.1 forms a cluster. A cluster of sufficient size (typically $N_{L1} \geq 5$) is selected together with all L0 hits within $2.2 \mu\text{s}$ the first and the last L1 hit. This value was chosen since it corresponds to the time needed by a relativistic muon to traverse the detector.

In addition to this first level selection, dedicated triggers are applied. We describe the two main filter algorithms used for the second level of events selection:

- **3N trigger.** The condition imposed by Equation 4.1 becomes stricter if the direction of the muon track is assumed. The 3N trigger tries a number of muon track directions

4. Simulation and reconstruction

looking for clusters of hits in a time window compatible with the Cherenkov emission. Since the direction of the muon is not known, the solid angle is divided in a grid with a spacing of about 10° . The arrival time t_i of a Cherenkov photon emitted by a muon is:

$$t_i = t_0 + \frac{1}{c} \left(z_i - \frac{r_i}{\tan(\theta_C)} \right) + \frac{1}{v_g} \frac{r_i}{\sin(\theta_C)}, \quad (4.2)$$

where z is the distance along the muon, θ_C is the Cherenkov angle, v_g the group velocity of light in water, r_i is the distance of closest approach between the muon and the PMT and t_0 is the time when the muon was at $z=0$. The second term in Equation 4.2 describes the time that it takes to the muon to travel from the initial position to the position where the photons are emitted. The last term is the time needed by the photons to reach the PMT. Figure 4.1 illustrates the topology. Hence, the 3N trigger selects clusters with pairs of hits which follow the relation

$$|t_i - t_j| \leq \frac{z_i - z_j}{c} + \frac{R_{ij}}{c} \tan(\theta_C) + 20 \text{ ns}, \quad (4.3)$$

where R_{ij} is the distance between PMT_i and PMT_j perpendicular to the muon direction as shown in Figure 4.1.

- **T3 trigger.** The T3 trigger requires two disjunct clusters, each consisting of at least two L1 hits in three consecutive storeys within a specific time window. This time window is 100 ns in case that the two storeys are adjacent and 200 ns for next-to-adjacent storeys. A minimum number of T3 clusters is then required in a pre-defined time window. For example, for two T3 clusters (2T3) at least 4 L1 hits are needed.

For the analysis presented in this thesis we select events from either the 3N trigger or the 2T3 trigger.

4.1.1. Trigger efficiency

The performance of the trigger is usually expressed in terms of its efficiency. The trigger efficiency for the 3N and the 2T3 trigger algorithms as a function of the neutrino energy is shown in Figure 4.2. It is defined as the ratio between the number of triggered events and the total number of reconstructed events. It is derived using a Monte Carlo sample which simulates the data taking period 2007-2010.

Figures 4.3 (atmospheric neutrinos) and 4.4 (E_ν^{-2} neutrinos) shows the trigger efficiency as a function of different reconstruction parameters: the neutrino zenith angle, θ_ν , the number of hits, N_{hits} , and the reconstruction variable Λ (see Section 4.3 for its definition).

For atmospheric neutrinos, the efficiency of the 2T3 trigger is on average in the range 70%-80% while the 3N trigger has a better efficiency at higher energies. A similar behaviour is seen for astrophysical neutrinos.

The 3N trigger efficiency for astrophysical neutrinos is higher than for atmospheric neutrinos. For the 2T3 trigger instead, atmospheric and astrophysical neutrinos are selected with roughly the same efficiency.

The trigger efficiency for the 3N and 2T3 trigger algorithms for both atmospheric and signal neutrinos is also summarised in Table 4.1.

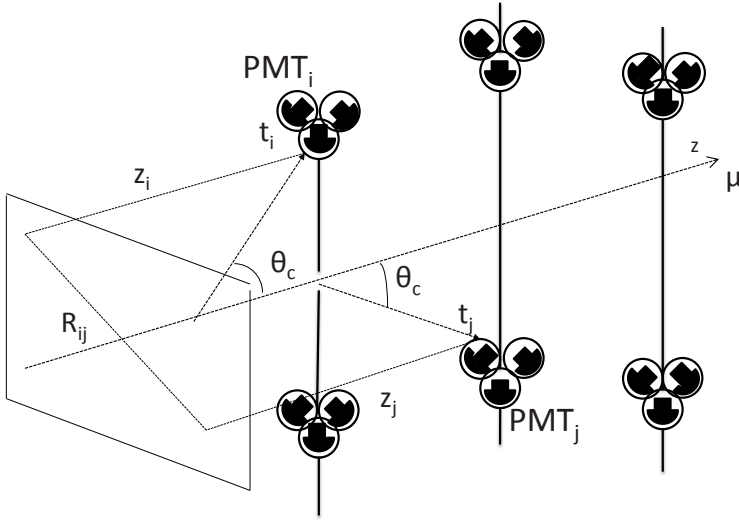


Figure 4.1.: Schematic view of a muon traversing the detector.

	atm. ν	$E_\nu^{-2}\nu$
Triggered events	100%	100%
3N events	66%	87%
2T3 events	84%	78%
3N only	14%	21%
2T3 only	33%	11%

Table 4.1.: Trigger efficiency for a Monte Carlo sample of atmospheric (second column) and signal (last column) neutrinos simulating the data taking period 2007-2010. The last two rows show the percentage of 3N (2T3) triggered events which are not accepted by the 2T3 (3N) trigger algorithm respectively.

4.2. Monte Carlo simulation

The interpretation of the data requires an accurate Monte Carlo (MC) simulation, which is used to understand the background contamination. MC simulations are also required to determine the acceptance and the angular resolution of the detector, since in the absence of a source of known size and intensity these quantities cannot readily be measured.

The MC simulation for the ANTARES detector can be divided in two stages:

- **Event generation.** Primary particles are generated at the top of the atmosphere (muons) or in a cylinder surrounding the detector (neutrinos) according to certain physical models.

4. Simulation and reconstruction

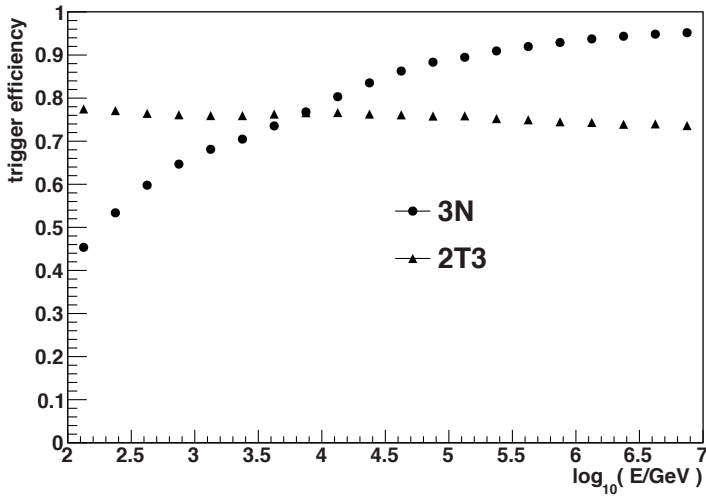


Figure 4.2.: Trigger efficiency for the 3N and 2T3 trigger algorithms defined as the ratio between the number of triggered events and the total number of reconstructed events as a function of the neutrino energy. A simulated sample of atmospheric neutrinos corresponding to the period of data taking 2007-2010 is used.

- **Light propagation and detector simulation.** The emission of Cherenkov light and the production of secondary particle showers is simulated in this phase. Then, the response of the detector to Cherenkov photons is simulated by taking into account the PMTs response, the electronic of the LCM and the triggers logic.

4.2.1. Event generation

The first step in the simulation chain is the event generation. Both neutrinos (atmospheric and cosmic) and muons are generated.

Neutrinos

Muon neutrino events are simulated using the GENHEN v6r3 [134] package. A large number of interactions¹ is generated within a cylinder around the detector. The size of this cylinder is chosen so that all the neutrinos which can produce a detectable muon inside the detector are simulated. Thus, the maximal muon range and the highest neutrino energy generated ($E_{\nu}^{\max} = 10^8$ GeV) are taken into account. Typically, this cylinder is 25 km in radius and height. Charged current interactions are simulated at this stage. The CTEQ6 parton distribution functions [109] are used for the cross section calculations. The probability for a neutrino to survive while traversing the Earth is given by Equation 1.23.

¹for the analysis presented in this thesis 5×10^8 neutrinos and anti-neutrinos for each run were simulated.

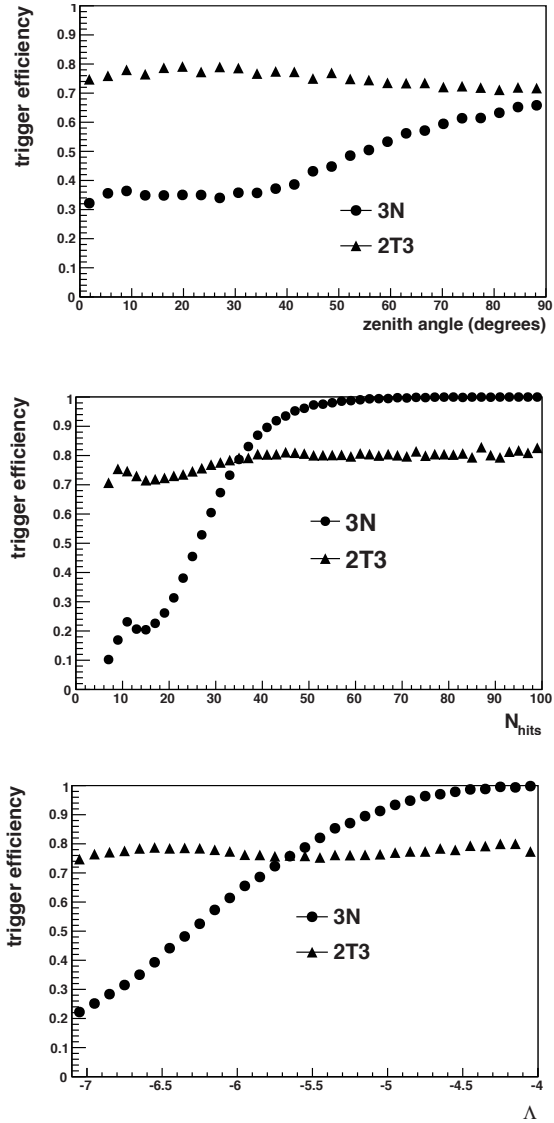


Figure 4.3.: Trigger efficiency for the 3N and 2T3 trigger algorithms defined as the ratio between the number of triggered events and the total number of reconstructed events as a function of the following parameters (from top to bottom): neutrino zenith angle, number of hits and Δ . A simulated sample of atmospheric neutrinos corresponding to the period of data taking 2007-2010 is used.

4. Simulation and reconstruction

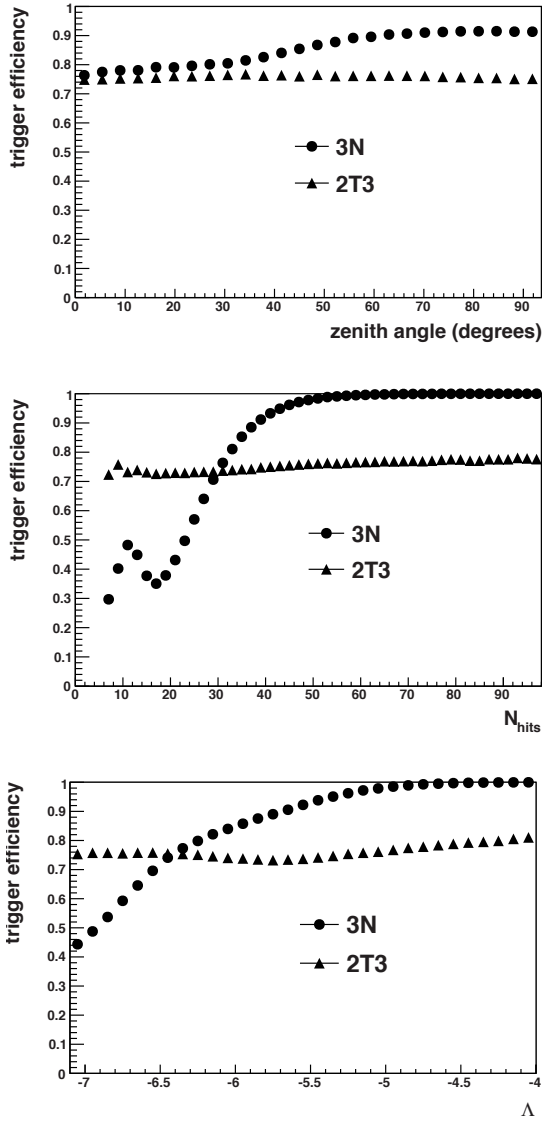


Figure 4.4.: Same as Figure 4.3 but for signal neutrinos with a spectrum proportional to E_ν^{-2} .

As was mentioned in Section 1.2.3, this probability is taken into account in the event rate calculations. The Earth density used is the Preliminary Reference Earth Model [135]. It is shown in Figure 4.5.

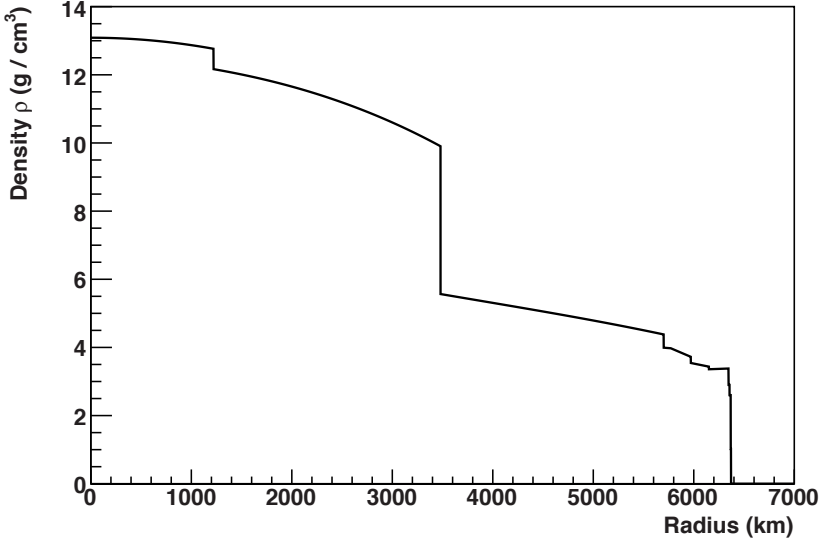


Figure 4.5.: Density profile of the Earth in the Preliminary Earth Model [135].

The neutrino directions are uniformly generated in the cosine of the zenith angle, in the range $[\cos \theta_{\min} = -1, \cos \theta_{\max} = 1]$ and in the azimuth angle in the range $[0, 2\pi]$. The generated energy follows a power law spectrum proportional to $E_\nu^{-\gamma}$, where γ is typically 1.4. The minimum and the maximum generated energies are respectively 10^2 and 10^8 GeV. In this way, roughly the same interacting neutrinos are simulated for each energy decade. It is custom to "weight" the events in order to simulate different neutrino fluxes. Hence, the same sample of generated events can be used to simulate atmospheric and various astrophysical neutrino fluxes. A generation weight, w_{gen} , is defined as:

$$w_{\text{gen}} = V_{\text{gen}} \cdot t_{\text{gen}} \cdot I_\theta \cdot I_E \cdot E^\gamma \cdot \sigma(E_\nu) \cdot \rho \cdot N_A \cdot P_{\text{Earth}} \quad (4.4)$$

where V_{gen} is the generation volume, $I_\theta = 2\pi \times (\cos(\theta_{\max}) - \cos(\theta_{\min}))$ is the angular phase space factor, $I_E = (E_{\max}^{1-\gamma} - E_{\min}^{1-\gamma}) / (1 - \gamma)$ is the energy phase space factor, $\rho \cdot N_A$ the number of target nucleons per unit volume and t_{gen} the interval of time simulated (usually a year). The simulation of a particular neutrino flux, $\phi^{\text{test}}(E_\nu, \theta_\nu)$, is done by re-weighting all the events in each energy and zenith bin by the factor $\phi^{\text{test}}(E_\nu, \theta_\nu) \cdot w_{\text{gen}}$.

For the analysis presented in this thesis, events are weighted according to the Bartol flux [55] for atmospheric neutrinos up to 100 TeV [136]. An energy spectrum proportional to E_ν^{-2} is adopted for the signal neutrinos unless stated otherwise.

The propagation of the muon from the neutrino interaction vertex to the so-called "can" is simulated with the MUSIC [137] package. The "can" is a cylinder which surrounds the detector for 2-3 light attenuation lengths. The Cherenkov light emitted by particles outside the can cannot reach the detector and therefore does not need to be simulated. The can

4. Simulation and reconstruction

and the detector geometry for event generation are shown in Figure 4.6.

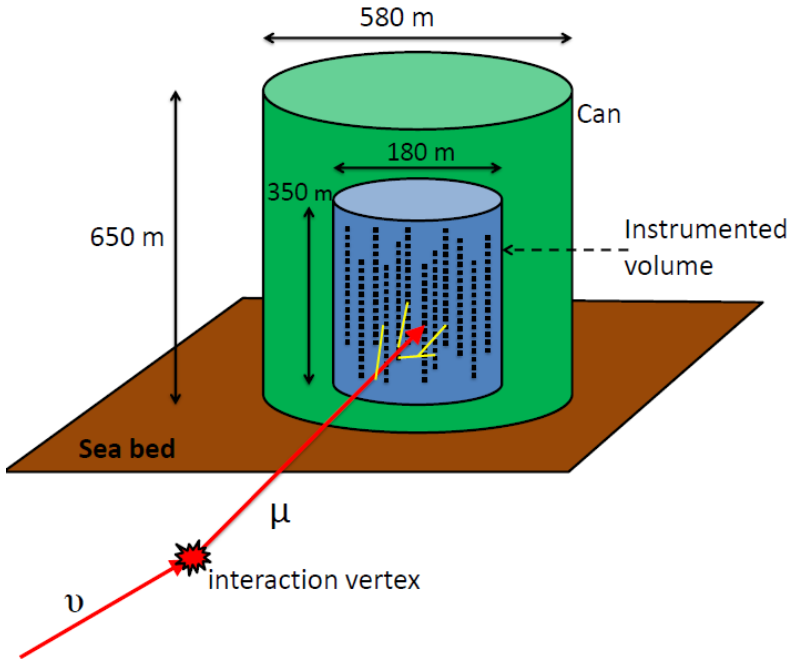


Figure 4.6.: Detector geometry for the event generation.

Atmospheric muons

Atmospheric muons events are simulated with MUPAGE v3r5 [138], which uses parametric formula to describe the flux, the angular distribution and the energy spectrum of underwater muon bundles of any multiplicity [139]. Events can be simulated for depths between 1.5 and 5 km w.e. and for zenith angles smaller than 85 degrees. The output of the program contains the values of the position, direction and energy of the muons at the can surface.

4.2.2. Light propagation and detector simulation

Light propagation

Particles are propagated inside the can using consecutively the GEASIM v4r10 [140] and the KM3 v3r7 [141] programs which are both based on the GEANT package [142].

Full GEANT tracking of hadronic showers is performed by GEASIM. For each particle, the arrival time of the Cherenkov light incident on the OMs is computed. The attenuation of the light is included, but the photon scattering is not simulated. The relative orientation of the PMTs with respect to the Cherenkov cone and the OM angular acceptance are included at this stage.

KM3 simulates the propagation of the muons in steps of 1 m. Due to the very large number of secondary electrons at high energies, the tracking of all the electromagnetic showers and the photons would require a lot of CPU time. KM3 avoids this problem by using photon tables which store the number and the arrival time of hits on OMs for different distances, positions and orientations of the OMs with respect to the track. Absorption and scattering of the light in water are both taken into account.

Detector simulation

The response of the detector is simulated with the TriggerEfficiency program [132] which adds of optical background hits to those produced by neutrinos or muons. It also simulates the electronics and the trigger algorithms.

Optical background hits are generated according to a Poisson probability distribution based on measured rates in order to take into account all the background contributions (radioactive decay and biological activities) for each run. In this way, the data taking conditions of all runs are reproduced. The condition of the detector, such as the fraction of inactive OMs due to high rate veto, are also reproduced. The electronics response is simulated by summing the number of photons detected during the time window of signal integration in the ARS chip (~ 40 ns). In order to take into account the time resolution for single electronic signals, typically 1.3 ns, the hit times are smeared with a Gaussian function with width

$$\sigma = \frac{1.3}{\sqrt{N_\gamma}} \text{ ns}, \quad (4.5)$$

with N_γ the number of detected photons. It was found [143] that the resulting distribution differs from the real distribution of the TTS obtained by measuring the time response of a 10 inch PMT to a single photo-electron. This discrepancy affects the agreement between data and Monte Carlo as will be explained in Section 5.1.

For each ARS, the simulated deadtime is 250 ns.

The simulation of the charge resolution of signal hits is done using a Gaussian distribution with mean 1 (1 photoelectron for a single photon) and width of 0.3 p.e. The simulation of the charge distribution of the random background is obtained from data. In the TVC calibration, the walk effect is taken into account.

After this stage, the same trigger algorithms used for the corresponding data runs are applied.

4.3. Track reconstruction

The reconstruction algorithm estimates the direction and the position of the muon with a multi-step fitting procedure [133]. The initial steps provide a starting point for the final maximisation of the track likelihood. The likelihood is defined as the probability density function of the observed hit time residuals r , given the track parameters. The time residual r_i is the difference between the observed and theoretical hit time for the assumed track parameters:

$$r_i = t_i - t_i^{th}. \quad (4.6)$$

4. Simulation and reconstruction

The distribution of the hit time residuals for reconstructed neutrino tracks is shown in Figure 4.7. The peak around zero is due to Cherenkov photons emitted by a muon and detected by the OMs in the absence of scattering. Thus, their arrival time is mostly affected by the TTS of the PMT and by dispersion. The tail of the distribution is caused by scattered photons and photons from secondary electrons. Optical background photons produce a flat distribution of time residuals.

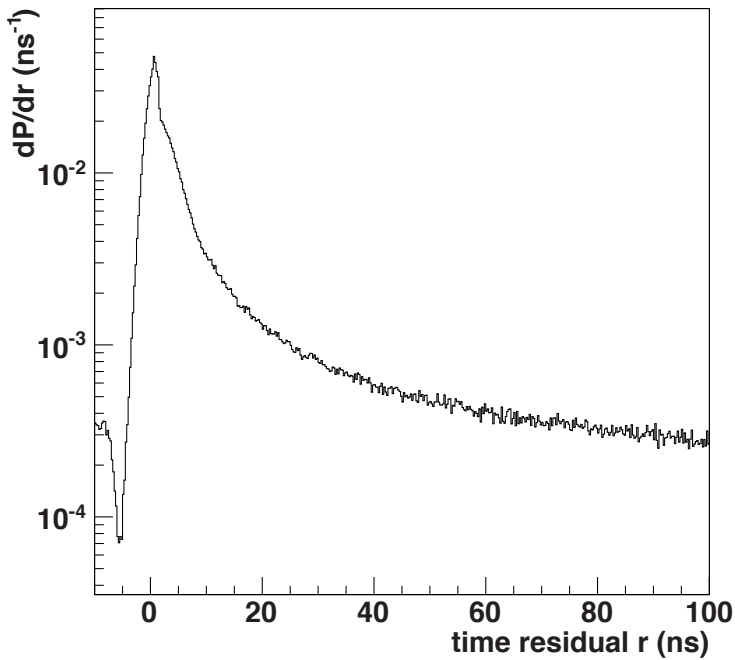


Figure 4.7.: Distribution of the reconstructed hit time residual for simulated neutrinos.

The track reconstruction starts with a linear fit through the positions associated with the hits with the hit time as independent variable. The distance of the muon track from the OM is estimated using the amplitude information and the orientation of the PMT. It is expected that a PMT recording a hit with high amplitude is located close to the track. This leads to the following relation:

$$\mathbf{y} = \mathbf{H}\Theta, \quad (4.7)$$

where $\mathbf{y} = [x_1, y_1, \dots, z_n]$ is the vector of the hit positions, $\Theta = [p_x, d_x, p_y, d_y, p_z, d_z]^T$ is

the vector containing the track parameters and \mathbf{H} is a matrix which contains the hit times:

$$\mathbf{H} = \begin{bmatrix} 1 & ct_1 & 0 & 0 & 0 & 0 \\ 0 & 0 & 1 & ct_1 & 0 & 0 \\ 0 & 0 & 0 & 0 & 1 & ct_1 \\ 1 & ct_2 & 0 & 0 & 0 & 0 \\ 0 & 0 & 1 & ct_2 & 0 & 0 \\ 0 & 0 & 0 & 0 & 1 & ct_2 \\ \vdots & \vdots & \vdots & \vdots & \vdots & \vdots \\ 0 & 0 & 0 & 0 & 1 & ct_n \end{bmatrix} \quad (4.8)$$

An analytical χ^2 minimisation is applied to estimate the track parameters, $\hat{\Theta}$:

$$\chi^2 = [\mathbf{y} - \mathbf{H}\hat{\Theta}]^T \mathbf{V}^{-1} [\mathbf{y} - \mathbf{H}\hat{\Theta}], \quad (4.9)$$

with \mathbf{V} the error covariance matrix which contains the error estimates on the hit positions.

The second step of the reconstruction algorithm is the M-estimator fit. M-estimators [144, 145] maximise some function g (in this case $g(r)$) and can be considered as more general cases of maximum likelihood fits. The function maximised by the M-estimator is

$$g = \sum_i g(r_i) = \sum_i -2\sqrt{1 + r_i^2/2} + 2, \quad (4.10)$$

where the sum runs over all the hits with time residuals from -150 ns to 150 ns and distances smaller than 100 m from the first track fit result are used..

It has been found that the M-estimator fit is not as accurate as a maximum likelihood fit but it is less sensitive to the quality of the starting point.

The third step consists of a maximum likelihood fit. Hits are selected if their residuals are in the range $[-0.5 \times R, R]$ where R is the root mean square of the residuals used for the M-estimator fit. Coincidence hits are also selected. At this stage, a simplified version of the full likelihood is used.

Both the M-estimator and the maximum likelihood fit are repeated using nine different starting points to further increase the probability of finding the global minimum.

The last step is a maximum likelihood fit with an improved likelihood function. This final likelihood function uses parametrisations for the probability density function (PDF) of the signal hit time residuals, derived from simulations. The PDF also takes into account hits arriving late due to Cherenkov emission by secondary particles or light scattering. The probability of a background hit is also included.

The quality of the track fit is quantified by the variable

$$\Lambda \equiv \frac{\log L^{\max}}{N_{\text{hits}} - 5} + 0.1 \times (N_{\text{comp}} - 1) \quad (4.11)$$

where L^{\max} is the maximum value of the likelihood, $N_{\text{hits}} - 5$ is the number of degrees of freedom which is the number of hits used in the fit, N_{hits} , minus the number of fit parameters. N_{comp} is the number of times the repeated initial steps of the reconstruction

4. Simulation and reconstruction

converged to the same result. In general, $N_{\text{comp}} = 1$ for most of the badly reconstructed events while it can be as large as nine for well reconstructed events. The coefficient 0.1 in Equation 4.11 was chosen to maximise the separation in Λ between signal and mis-reconstructed downgoing muons.

In general, well reconstructed events have larger Λ . The Λ variable can thus be used to reject badly reconstructed events, in particular mis-reconstructed atmospheric muons.

Figure 4.8 shows the distribution of the reconstruction angle, α , i.e. the angle between the generated neutrino and the reconstructed muon direction, is plotted. After requiring a cut $\Lambda > -5.2$ most of the badly reconstructed events are rejected.

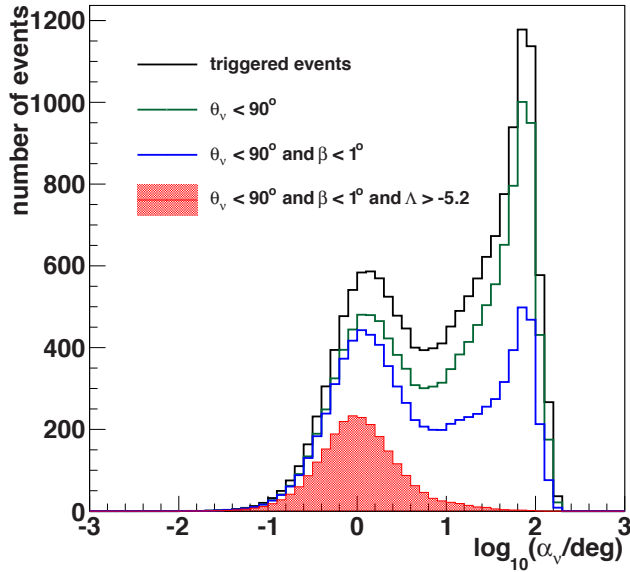


Figure 4.8.: Distribution of α , i.e. the angle between the generated neutrino and the reconstructed muon direction, for simulated atmospheric neutrinos before and after applying the event selection cuts described in Section 6.2.

Figure 4.9 (top) shows the reconstruction angle α as a function of the Λ variable for simulated atmospheric neutrinos. The bottom plot shows a profile distribution [146] of these two variables. The error bars represent the standard deviation of the α distribution. A comparison between atmospheric and E^{-2} neutrinos is shown for the same quantities.

Error estimates of the track direction are provided by the reconstruction algorithm under the assumption that the likelihood function near the fitted maximum follows a multivariate Gaussian distribution. The error estimates, which are elements of the error covariance matrix, are computed from the second derivatives of the likelihood function at the fitted

maximum:

$$[\mathbf{V}^{-1}]_{ij} = -\frac{\partial^2 \log(L)}{\partial x_i \partial x_j} \quad (4.12)$$

where \vec{x} is the vector of track parameters: $\vec{x} = (p_x, p_y, p_z, \theta, \phi)$. The estimated error on the zenith and azimuth angles, $\hat{\sigma}_\theta$ and $\hat{\sigma}_\phi$, are of particular interest. Figure 4.10 shows the pull distributions for the zenith (top) and azimuth (bottom) angles. A pull is defined as the ratio between the true error on a variable and its error estimate. Ideally, the pull distribution should be Gaussian with mean zero and width $\sigma = 1$. As can be seen from Figure 4.10 the width of the two pulls is larger than one. This is due to the fact that the PDF is not a perfect description of the residuals in the Monte Carlo simulations. This is partially due to the 2 ns smearing which will be discussed in details in Section 5.1.

From the estimated errors on the zenith and azimuth angles, it is possible to compute the estimate of the error on the direction of the muon track, β , which will be used to reject mis-reconstructed atmospheric muons:

$$\beta = \sqrt{\sin^2(\hat{\theta})\hat{\sigma}_\phi^2 + \hat{\sigma}_\theta^2}. \quad (4.13)$$

The distribution of β is shown in Figure 6.9.

4. Simulation and reconstruction

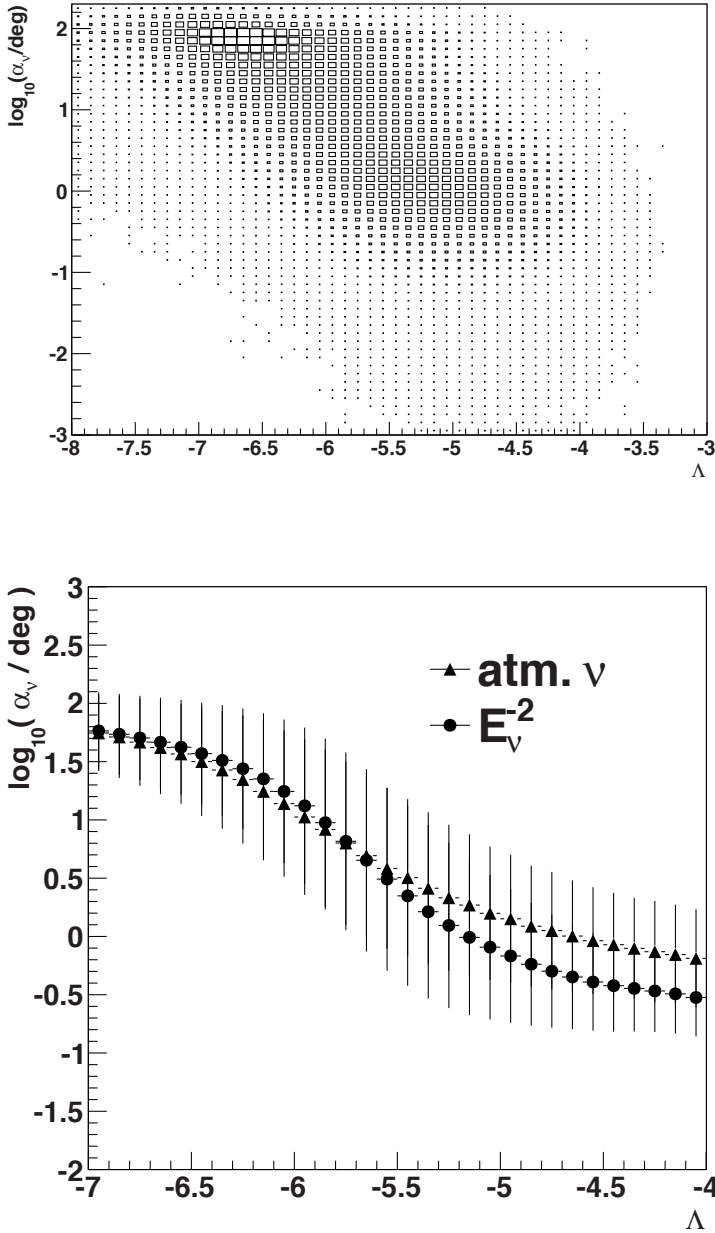


Figure 4.9.: Top: reconstruction angle α vs Λ for atmospheric neutrinos. Bottom: Profile distribution of these two quantities. A comparison between atmospheric and E^{-2} neutrinos is shown.

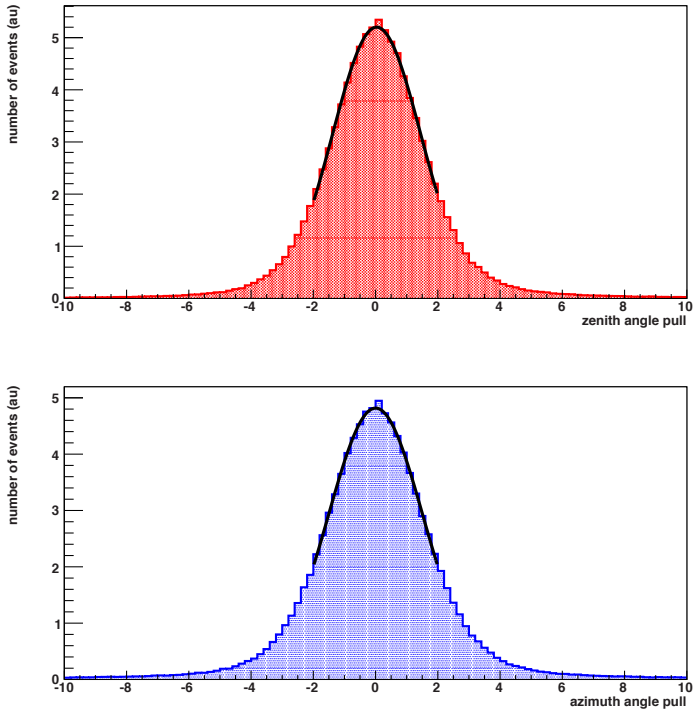


Figure 4.10.: Pull distributions for the zenith (top) and azimuth (bottom) angle for a simulated sample of neutrinos. A quality cut $\Lambda > -5.2$ is applied. A Gaussian function between -2 and 2 is used to fit the distribution. The width of the Gaussian is $\sigma = 1.41$ for the zenith angle pull and $\sigma = 1.51$ for the azimuth angle pull.

